



Cite this: *Dalton Trans.*, 2016, **45**, 14499

Received 11th May 2016,  
Accepted 14th July 2016  
DOI: 10.1039/c6dt01857b  
www.rsc.org/dalton

## Insights into small molecule activation by multinuclear first-row transition metal cyclophanates

David M. Ermert and Leslie J. Murray\*

The rational design of trimetallic transition metal clusters supported by a trinucleating cyclophane ligand,  $L^{3-}$ , and the reactivities of these complexes with dinitrogen and carbon dioxide are discussed. Emphasis is placed on the differences in the observed reactivity between these trimetallic cyclophane complexes and that of the mono- and dinuclear transition metal compounds.

### Introduction

Bioavailable nitrogen (*e.g.*, ammonia) is crucial to life on earth as N atoms are principal building blocks of proteins and nucleic acids.<sup>1</sup> Although the planet's atmosphere is predominantly composed of  $N_2$  gas (78%),<sup>2</sup> the strong triple bond between the two N-atoms renders  $N_2$  as chemically-inert. However, the conversion of dinitrogen to ammonia is thermodynamically favourable ( $\Delta H^\circ = -92.22 \text{ kJ mol}^{-1}$ ;  $\Delta G^\circ = -16.48 \text{ kJ mol}^{-1}$ ) albeit kinetically limited under ambient conditions.<sup>3</sup> Currently, atmospheric dinitrogen is converted to ammonia in two principle systems:  $N_2$  fixation by the nitrogenase family of enzymes in *Rhizobacter*,<sup>1,4</sup> and industrially using the Mittasch catalyst in the Haber–Bosch process (HBP).<sup>5</sup> The HBP requires high temperature and pressure of  $N_2$  and  $H_2$ , which in part accounts for the large energy demands ( $\sim 1\%$  of global energy consumption) of this process.<sup>5a,6</sup> The HBP is exceptionally energy efficient on large scale production, but it unfortunately relies on fossil fuels (inc. dihydrogen derived from methane). Such centralized production inherently incurs distribution costs, which can be prohibitively expensive depending on the end user's location (*e.g.*, sub-Saharan Africa). Discovering alternative strategies for decentralized  $N_2$  fixation are thus critical given the importance of ammonia as an N source for crop plants and as a synthon for commodity chemical production. These approaches can operate at lower efficiencies provided that they utilize renewable energy sources (*e.g.*, solar) to drive the chemistry.

The biological method for  $N_2$  fixation is indeed decentralized with “local” and on-demand  $NH_3$  production afforded by the symbiotic relationship between the host plant and the bac-

teria. This process is energetically inefficient, consuming 16 equivalents of ATP per  $N_2$  molecule,<sup>1</sup> and it is difficult to extend this approach to a broad range of crop plants; transposing the genes or recreating the symbiotic relationships remain unrealized.<sup>7</sup> The nitrogenase enzymes utilize a polynuclear iron sulfur cluster of the type  $Fe_7S_9MC$ , where  $M = Mo, Fe,$  or  $V$ , as the active site for  $N_2$  reduction (Fig. 1).<sup>8</sup> These enzymes operate under ambient temperature and pressure, suggesting that similar small scale low temperature synthetic systems can be viable alternatives to the HBP. Inspired in part by the multi-metallic nature of the nitrogenase cofactors and more broadly by the plethora of multimetallic cofactors that activate small molecule substrates (*e.g.*,  $Cu_z$  in nitrous oxide reductase and  $NiFe_4S_8$  cluster in NiFe carbon monoxide dehydrogenase),<sup>9</sup> we

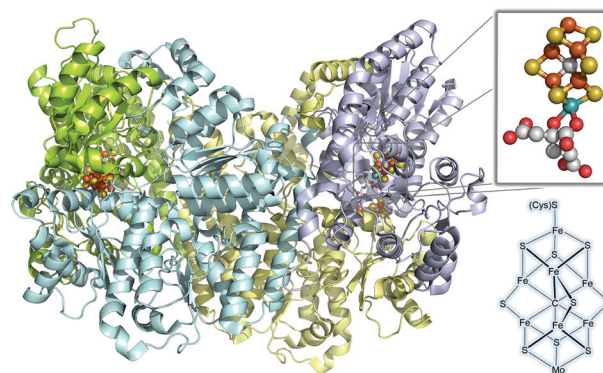
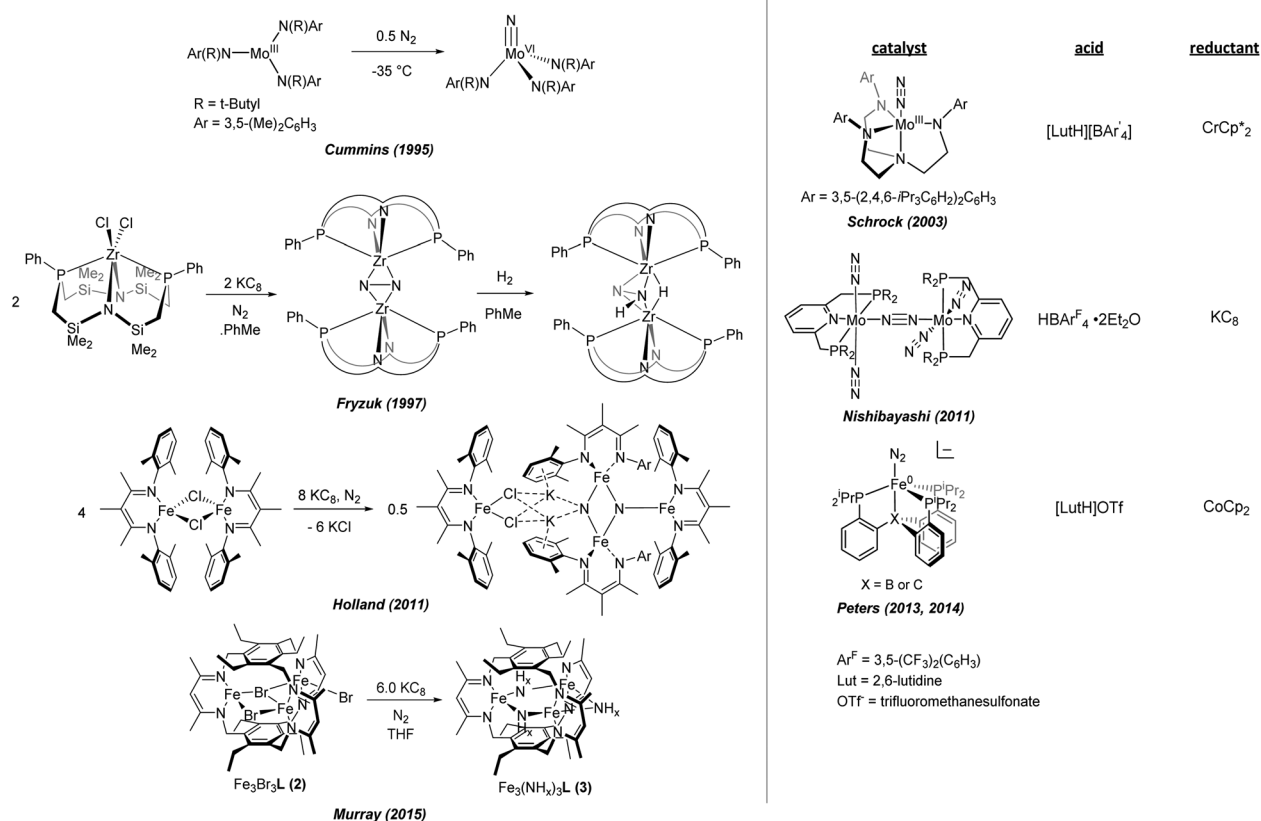


**Fig. 1** Crystal structure of the MoFe protein (left), the iron-molybdenum cofactor or FeMo-co (top right), and a schematic representation of the cofactor (bottom right). The  $\alpha$ ,  $\beta$ ,  $\gamma$ , and  $\delta$  subunits are represented ribbon diagrams in green, teal, purple, and yellow, with the metal cofactors depicted as spheres. Carbon, oxygen, sulfur, iron, and molybdenum atoms are shown in grey, red, yellow, orange, and teal spheres. Crystallographic coordinates obtained from PDB entry 3U7Q.



**Scheme 1** Selected stoichiometric and catalytic systems for N<sub>2</sub> activation.

and others<sup>10</sup> have targeted multimetallic complexes as possible reaction sites for the dinitrogen activation and fixation.

Since Senoff and Allen reported the first N<sub>2</sub>-bound transition metal complex, a large number of dinitrogen complexes and systems that activate N<sub>2</sub> by partial or complete scission of the N≡N bond have been reported.<sup>11</sup> Cummins and Laplaza described the rapid cleavage of atmospheric dinitrogen by a three-coordinate molybdenum(III) complex at −35 °C to form two terminally-bound Mo(VI) nitrides (Scheme 1).<sup>12</sup> Shortly thereafter, Fryzuk and coworkers reported a Zr(IV) system that cleaves the N≡N triple bond of dinitrogen to form a dizirconium-hydrazide which generates a Zr<sub>2</sub>(μ:η<sup>2</sup>-N<sub>2</sub>H)(μ-H) imido complex.<sup>13</sup> The Schrock group was the first to report catalytic reduction of N<sub>2</sub> to NH<sub>3</sub> by a discrete monometallic complex using stepwise addition of a reductant and proton source.<sup>14</sup> Nishibayashi and coworkers demonstrated that a PNP-pincer supported Mo(III) chloride binds N<sub>2</sub> upon reduction and catalytically generates NH<sub>3</sub> in the presence of a mild reductant and acid.<sup>15</sup> Iron systems competent for N<sub>2</sub> cleavage have similarly been reported. Tyler demonstrated that a low-spin mono-iron complex that binds atmospheric dinitrogen would subsequently liberate ammonia and hydrazine upon addition of a strong acid.<sup>16</sup> More recently, Rodriguez *et al.* communicated that reduction of a (β-diketiminato)iron(II) dimer under an N<sub>2</sub> atmosphere affords a self-assembled tetrairon di(nitride) complex.<sup>17</sup> The two nitride ligands can be released as

ammonia by treating the cluster with a proton source. Finally, Peters and coworkers reported the first catalytic systems employing iron, in which a family of tripodal iron complexes allow for detailed examination of N<sub>2</sub>-binding, formation of terminal nitrides, N–H bond formation, and NH<sub>3</sub> production.<sup>18</sup> In all of these cases, the focus is primarily on the design of monometallic complexes, despite evidence suggesting that multiple metals may be involved in N<sub>2</sub> scission.

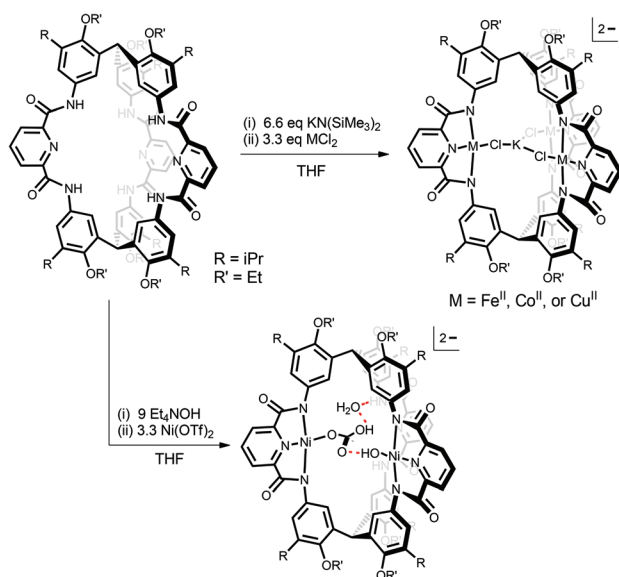
### Macrocycles as ligands for multimetallic compounds

In considering the design of multimetallic compounds, one can develop ligands that either promote or preclude direct metal–metal interactions. In the case of direct metal–metal interactions, Berry,<sup>10j,k</sup> Betley,<sup>10f-h</sup> Lu,<sup>10a-c</sup> and Thomas,<sup>10d,e</sup> among others have made important and exciting contributions and demonstrated profound and diverse reactivities. By inhibiting direct metal–metal interactions, however, the effect of metal ion proximity can be directly evaluated by comparing the reactivity of the monometallic complexes with that of the multimetallic congeners. In addition, this design approach simplistically treats the multimetallic complex as an aggregate of individual monometallic units in which the relative orientation of the frontier orbitals of each fragment and the distance between the metal ions can be controlled and varied. The ligand in this approach must enforce a narrow range of metal–metal distances to favour substrate binding,

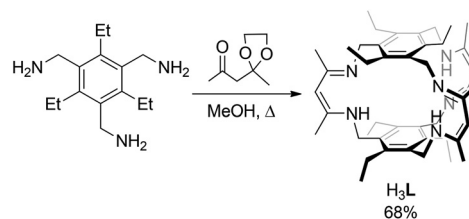
but prevent metal–metal bond formation. One family of organic compounds that meet these criteria are macrobicycles, which we<sup>19</sup> and others<sup>20</sup> have employed extensively as ligands for tri- and di-metallic complexes.

Our first generation macrobicyclic ligand utilized derivatized triphenylmethane fragments as caps and pyridine-2,6-dicarboxamide arms.<sup>19a,b</sup> Deprotonation of the six amides of this ligand followed by metalation afforded the corresponding trimetallic complexes with each metal held in the *N,N,N*-chelate of each arm (Scheme 2). The resultant complexes are predominantly anionic, however, with the fourth coordination site in the square plane occupied by a halide donor in all complexes except for the trinickel(II) species. Disappointingly, the accessible axial coordination sites of each metal in these complexes are not oriented towards the internal void space. Nonetheless, O-atom transfer (albeit ineffective) from iodobenzene to triphenylphosphine is possible using the tri(chloro-iron(II)) complex. In reactions using substoichiometric equivalents of base and acetonitrile, we were also able to access complexes in which the metal ions are coordinated by an *O,N,O*-chelate rather than the *N,N,N* one. More interestingly, dimetallic complexes could be readily accessed by varying the base in the reaction, which led to the discovery of CO<sub>2</sub> capture from ambient air by presumed terminal copper(II) and nickel(II) hydroxide species.

With these drawbacks in mind, the subsequent ligand design diverged from the triphenylmethane building block and instead utilized 1,3,5-tri(aminomethyl)-2,4,6-triethylbenzene. Ansyn and coworkers highlighted the preferential alternating up-down configuration as key for maximizing synthetic yields.<sup>21</sup> The ethyl groups should also allow for facile access of substrates to the central cavity. Indeed, the tris(pyri-



**Scheme 2** Synthesis of di- and trimetallic compounds using a tris(pyridine-2,6-dicarboxamide) cryptand. Hydrogen bonds in the dinickel species are depicted as red dashed lines. Adapted from ref. 19a and b.

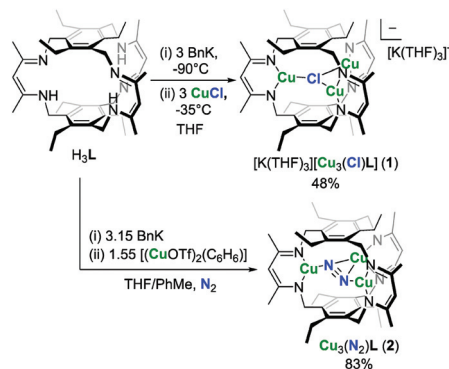


**Scheme 3** Synthesis of tris( $\beta$ -diketimine) cyclophane, H<sub>3</sub>L. Adapted from ref. 19c.

dine-2,6-dicarboxamide) cyclophane of this cap functions as an organic receptor with rapid diffusion of acetate and other anions into the central cavity.<sup>22</sup> The  $\beta$ -diketiminate was selected as the donor arm because the extensive literature precedent on the reactivity of mononuclear ( $\beta$ -diketiminato)metal complexes can be contrasted to the that observed for metal complexes of this cyclophane (Scheme 3).<sup>23</sup> Similar metalation strategies afford the expected trimetallic complexes.<sup>19c,d,k</sup> The chemistry of these compounds will be the primary focus of this Perspective.

### N<sub>2</sub> binding and cleavage by trimetallic cyclophanates

The tricopper(I) cyclophanate complex was an early target because of our interest in modelling the active site of multicopper oxidases (MCOs) and other multicopper active sites in biological systems.<sup>24</sup> Addition of benzylpotassium to solutions of H<sub>3</sub>L in THF generate the tripotassium salt (K<sub>3</sub>L) which, upon metalation with cuprous chloride *in situ*, yielded the anionic complex [Cu<sub>3</sub>( $\mu$ -Cl)L]<sup>-</sup> (**1**) (Scheme 4).<sup>19d</sup> From the crystal structure, the copper–copper distances in **1** range from 4.1–5.0 Å and are comparable to those observed in the tricopper active site of MCOs.<sup>25</sup> Our initial attempts to probe the reactivity of this complex with dioxygen were challenging; the reaction kinetic traces were complex and not readily modelled. We sought to remove the internal chloride from the complex, as chloride dissociation could contribute to the observed complexity. Using a similar metalation strategy but with a larger counter anion for the copper(I) source (*i.e.*, CuBr or



**Scheme 4** Synthesis of tricopper(I) clusters [K(THF)<sub>3</sub>][Cu<sub>3</sub>(Cl)L] (**1**) and Cu<sub>3</sub>(N<sub>2</sub>)L (**2**). Adapted from ref. 19d and e, respectively.

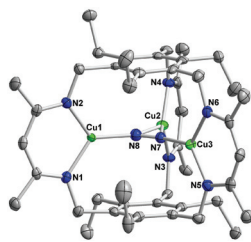


Fig. 2 Crystal structure of  $\text{Cu}_3(\text{N}_2)\text{L}$  (**2**) at 60% thermal ellipsoids. C, N, and Cu atoms depicted as gray, blue, and green ellipsoids. H-atoms and solvent molecules are omitted for clarity. Adapted from ref. 19e.

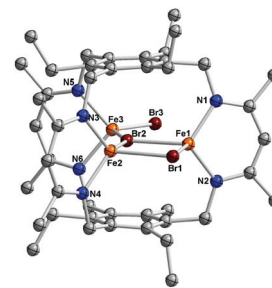


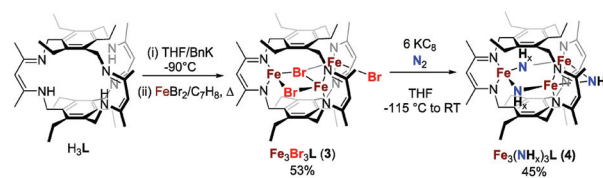
Fig. 3 Crystal structure of  $\text{Fe}_3\text{Br}_3\text{L}$  (**3**) at 90% thermal ellipsoids. Hydrogen atoms and solvent molecules have been omitted for clarity. C, N, Fe, and Br atoms depicted as gray, blue, orange, and maroon ellipsoids, respectively. Adapted from ref. 19c.

$[\text{Cu}(\text{OTf})_2](\text{C}_6\text{H}_6)$ ), we were surprised to isolate a  $(\mu\text{-}\eta^1\text{:}\eta^2\text{:}\eta^1\text{-dinitrogen})\text{tricopper(i)}$  complex, **2** (Fig. 2).<sup>19e</sup> This compound represents the first molecular complex containing  $\text{Cu-N}_2$ ; previously,  $\text{Cu(i)-N}_2$  species have been observed in the gas phase or in copper(i)-doped porous solids.<sup>26</sup> The  $\text{N}\equiv\text{N}$  bond distances in **2** (1.0956(1)–1.0854(1) Å) are shorter than in free  $\text{N}_2$ , which seem to contradict the  $\text{N-N}$  stretching mode at  $1952\text{ cm}^{-1}$  – almost  $400\text{ cm}^{-1}$  lower in energy than that for free  $\text{N}_2$  – observed in resonance Raman spectra collected on  $\text{Cu}_3(\text{N}_2)\text{L}$ . In addition, DFT calculations on optimized structures of **2**, in which a methyl-for-ethyl substitution was employed for the arene caps, are consistent with minimal  $\pi$ -backbonding as evidenced by the computed  $\text{N-N}$  bond distance (1.125 Å) and the  $\text{N-N}$  vibrational frequency ( $2094\text{ cm}^{-1}$ ). Given these conflicting results, we noticed in DFT calculations that decreasing the size of the alkyl substituents on the ligand resulted in greater  $\text{N-N}$  activation. We, therefore, suggested that the  $\text{N-N}$  distance in the solid state may be influenced by crystal packing effects that force the complex to adopt a conformer with a lesser degree of  $\text{N}_2$  activation whereas the vibrational data reflect the greater flexibility in the solution state that allows the compound to sample conformers with a more activated  $\text{N}_2$  ligand. Fortuitously, the coordination mode of dinitrogen in the  $\text{Cu}_3(\text{N}_2)\text{L}$  complex bears strong resemblance to the computational model proposed by Cundari and Holland, in which the side-on coordination of a third iron(i) center was required for  $\text{N-N}$  bond scission. This tricopper(i)-dinitrogen complex can be thought of as a potential intermediate analog along the dinitrogen activation pathway by low valent ( $\beta$ -diketiminato)metal complexes.<sup>17,27</sup>

Part of the inspiration for the cyclophane design stemmed from Holland's work on  $\text{N}_2$  activation, and in particular, their report of dinitrogen activation upon reduction of a ( $\beta$ -diketiminato)iron(ii) chloride complex.<sup>17,28</sup> There, the  $\text{N}_2$  derived fragment is best described as three iron centers bridged by two nitride donors; thus, our ligand seemed to provide a direct route to probing if three iron atoms are competent for  $\text{N}_2$  bond scission. The triiron(ii) tri(bromide) complex,  $\text{Fe}_3\text{Br}_3\text{L}$  (**3**), could be readily accessed using our general protocol.<sup>19c</sup> Each  $\text{Fe(ii)}$  center in this compound is pseudo-tetrahedral, supported by the  $N,N$ -chelate of a  $\beta$ -diketiminato arm and two bromide ions (Fig. 3). Initially, three equivalents of potassium graphite were used to investigate  $\text{N}_2$  activation by **3**; we antici-

pated formally reducing each iron center to the monovalent state followed by a six electron reduction of  $\text{N}_2$  to generate a triiron(iii) di( $\mu$ -nitride) species. Surprisingly, the triiron complex,  $\text{Fe}_3(\text{NH}_x)_3\text{L}$  (**4**), was instead the observed product (Scheme 5). Subsequently, the reaction conditions were optimized to maximize the yield of  $\text{NH}_3$  released from acid hydrolysis of the product, which corresponded to 6 equiv. of  $\text{KC}_8$ . Curiously, dinitrogen reduction appears to funnel into the  $\text{Fe}_3(\text{NH}_x)_3\text{L}$  product and we remain unable to isolate complexes with fewer  $\text{N}_2$  derived N-atoms by starving the reaction of reducing equivalents. The degree of protonation of the  $\text{N}_2$  derived ligands is likely a mixture of amide and imide donors, leading to mixed valent compounds as determined from our Mössbauer spectra. The designed approach employed by us evidently leads to reactivity differences from the monometallic systems, strongly suggesting that we access distinct cooperative pathways as compared to the self-assembled monometallic system. The interplay between the limited conformations and the enforced orbital interactions in our complexes as compared to those for the monometallic system are undoubtedly important.

The notable differences in our result as compared to previous work are that all N-atom bridges are protonated, and that we incorporate *three* N-atoms.<sup>19f</sup> The proton source remains undetermined in this reaction, but we can exclude adventitious water on the glass surface and solvent protons. This was possible by evaluating the reduction products for reactions performed in silylated glassware and in deuterated solvents, respectively. Therefore, the ligand C-H bonds remain likely candidates of these protons. Protonation of transient nitrides as in our system likely tunes the reduction potential of



Scheme 5 Synthesis and reduction of  $\text{Fe}_3\text{Br}_3\text{L}$  (**3**). Adapted from ref. 19f.

the cluster, opening access to further reductive chemistry. Evidence in support of this hypothesis has recently been provided by Holland and coworkers as well as the surprisingly low one-electron redox process observed for  $\text{Fe}_3(\text{NH}_2)_3\text{L}$  ( $\sim -0.85$  V vs.  $\text{Fc}/\text{Fc}^+$ ).<sup>38,19h</sup>

The presence of a third N-donor implicates at least one intercluster step occurs during reduction of dinitrogen. Although the approach of two triiron complexes seems unlikely from a steric perspective, we were fortunate to obtain the solid-state structural solution of a dimeric product (5), which co-crystallized with 4 from a reaction (Fig. 4).<sup>19f</sup> The interdigitation of the ethyl substituents on the caps and the methyl groups on the diketiminate arms affords a suitable binding site for two  $\text{K}^+$  cation at the interface. The structure bears strong similarities to the  $\text{K}^+$  incorporation in other di-, tri-, and tetrairon compounds containing a bridging  $\text{N}_2$  or two  $\text{N}^{3-}$  donors.<sup>17,28</sup>

Evidence for an intercluster pathway brings in to question whether metal–metal interactions within a cyclophanate complex are important for  $\text{N}_2$  activation or if  $\text{N}_2$  undergoes bond cleavage only at the interface between two complexes (Scheme 6). The dibromo( $\mu_3$ -nitrido)triiron complex 7 could be an intermediate along an intercluster-only mechanism with

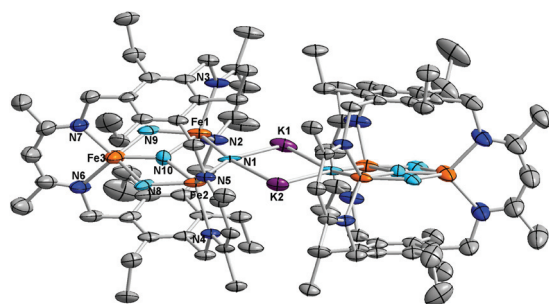


Fig. 4 Solid-State structural solution of 5 at 50% thermal ellipsoids. Hydrogen atoms and solvent molecules have been omitted for clarity. C, N, Fe, and K atoms depicted as gray, blue, orange, and purple ellipsoids, respectively. Bridging atoms modelled as nitrides are shown as light blue ellipsoids. Adapted from ref. 19f.

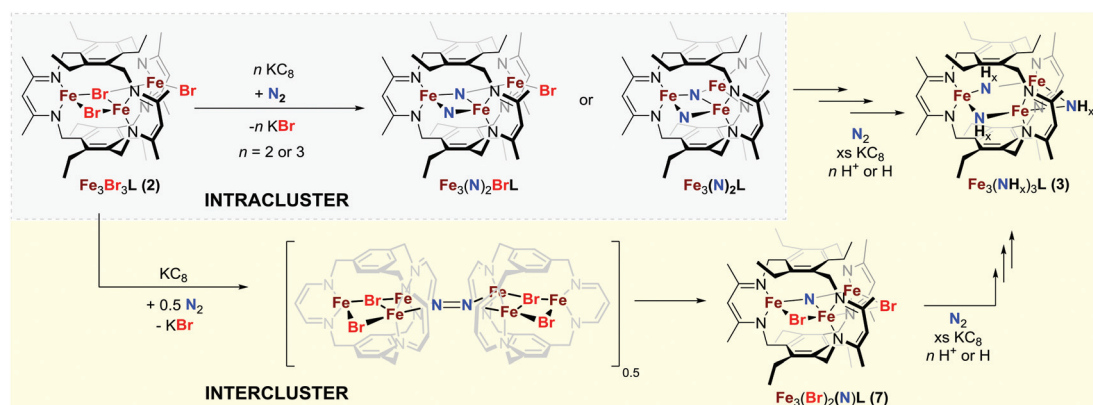


Scheme 7 Synthesis of  $\text{Fe}_3(\text{Br})_2(\text{N})\text{L}$  (7). Adapted from ref. 19h.

the reactivity of this species providing support for either pathway.  $\text{Fe}_3(\text{Br})_2(\text{N}_3)\text{L}$  (5) was prepared by substitution of one halide in 3 with azide (Scheme 7). Thermolysis of 5 in the solid state resulted in the loss of azide vibration ( $2082\text{ cm}^{-1}$ ) by IR spectroscopy and the isolation of 6 as an olive green solid. As for  $\text{Fe}_3\text{Br}_3\text{L}$ , there are no reversible redox couples observed in cyclic voltammograms of 6 up to  $-2.5$  V vs.  $\text{Fc}/\text{Fc}^+$ . Moreover, preliminary attempts to reduce dinitrogen by treating 6 with a strong reductant have been unsuccessful, independent of the number of equivalents of  $\text{KC}_8$  added. These data provide early support that the intracuster pathway is important for dinitrogen activation in our system. Admittedly, protons can tune the reactivity and electrochemical properties of these complexes and are not considered in attempts to reduce dinitrogen starting with 6; that is, coupling proton and electron delivery may turn-on the reactivity of 6 or reduced variants towards  $\text{N}_2$ .

### Substrate specific reactivity of hydride-bridged trimetallic complexes

The mechanism for dinitrogen reduction by FeMoco proposed by Hoffman, Seefeldt, and Dean relies on the reductive elimination of two iron hydrides to generate the reactive species that binds  $\text{N}_2$ .<sup>1,4b,29</sup> Relatedly, hydride complexes of various transition metals can readily eliminate  $\text{H}_2$  and subsequently bind  $\text{N}_2$ .<sup>30</sup> In essence, these hydride ligands mask low valent metal centers, and protecting reducing equivalents prior to reaction with dinitrogen. Photochemical or thermal reductive elimination occur in the di( $\mu$ -hydrido)dimetallic complexes sup-

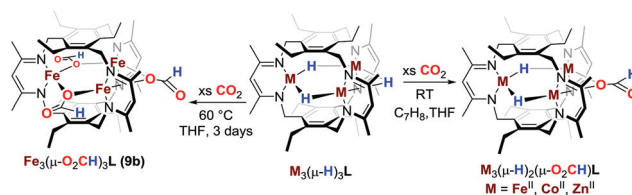


Scheme 6 Proposed inter- and intracuster pathways for dinitrogen cleavage upon chemical reduction of  $\text{Fe}_3\text{Br}_3\text{L}$  (3) in yellow and black backgrounds, respectively. Adapted from ref. 19h.

ported by  $\beta$ -diketiminates.<sup>28,31</sup> Hydride-decorated trinuclear transition metal clusters supported by our cyclophane were, therefore, a natural extension in our studies on dinitrogen activation. These metal hydride clusters could provide insight into the enzymatic reaction as well as the potential cooperative events on the iron face of the Mittasch catalyst during the Haber-Bosch process.

Reaction of  $M_3Br_3L$  (where  $M = Fe^{II}$  or  $Co^{II}$ ) with potassium superhydride generates the corresponding trihydride complex,  $M_3(\mu-H)_3L$  (where  $M = Fe^{II}$  and  $Co^{II}$ ).<sup>19i</sup> Neither thermal nor light-driven  $H_2$  reductive elimination could be accessed in these systems, and no reactivity with  $N_2$  was observed as expected. The inability to eliminate  $H_2$  is likely because the hydride-hydride distances are considerably longer (2.7608(1)–3.3670(2) Å) than in the dimeric compounds, and prevent the necessary orbital overlap to form the H–H bond. The order of dinitrogen binding and dihydrogen loss from some metal hydrides, however, is uncertain.<sup>32</sup> For FeMoco, one can envision  $N_2$  association instigating  $H_2$  loss rather than  $H_2$  elimination occurring prior to substrate binding.<sup>29</sup> We, therefore, began to survey a variety of substrates with the expectation that either hydride insertion or reductive elimination could be observed. To our surprise, IR and NMR spectra provided no evidence for reaction with benzonitrile, acetonitrile, benzaldehyde, acetone, or carbon disulphide. However, carbon dioxide cleanly reacts with both the triiron(II) and tricobalt(II) trihydrides over the course of several days at room temperature to afford the ( $\mu$ -1,1-formato)di( $\mu$ -hydride)trimetallic complexes (Fig. 5). In the case of the triiron trihydride complex, all three hydrides can be forced to insert into  $CO_2$  by using elevated temperatures to give the tri( $\mu$ -1,1-formate) complex, which was not observed for the cobalt congener (Scheme 8). This difference in reactivity between  $Co_3H_3L$  and  $Fe_3H_3L$  likely arises from the difference in the metal-hydride bond strengths.

The observed high specificity for  $CO_2$  was unprecedented, and the muted reactivities of the three hydrides donors in these complexes are unusual. A steric component to the substrate specificity is likely as substrates must navigate the narrow space between the two ethyl substituents, although electronic effects are also certainly present as suggested by the



Scheme 8 Reactivity of trimetallic trihydrides with  $CO_2$ .

contrasting reactivities of the Co and Fe systems. In order to probe the steric effects and to more rapidly screen substrates, we targeted the trizinc congener and employed NMR spectroscopy to evaluate reaction mixtures.<sup>19g</sup> In addition, zinc hydrides typically exhibit broad substrate functional group scope for hydride transfer, and changes to that reactivity profile in our system would likely arise from steric effects.<sup>33</sup> Here again, we observed no reactivity over a 24 h period for the nitrile and carbonyl substrates or  $CS_2$ . Even more surprisingly,  $Zn_3H_3L$  is unreactive towards protic solvents over the same time course, and is air-stable as a solid; NMR spectra for samples with added methanol or water are unchanged. This tolerance to protic solvents – in particular, water – and ambient moisture were previously unprecedented for zinc hydrides. As for the iron and cobalt clusters,  $Zn_3H_3L$  reacts readily with  $CO_2$  to generate the analogous formate-di(hydride) complex.

The causes of the high specificity for  $CO_2$  by these compounds remain unclear. One could envision that the ligand exerts strong size discrimination on substrates as suggested from the space-filling models of these complexes. Rotation of the ethyl groups is thermally accessible at room temperature and in solution, based on work by Anslyn, which would serve to further limit substrate access.<sup>21</sup> Such an argument rationalizes the lack of reactivity towards the tested nitrile and carbonyl substrates, but seems unlikely for  $CS_2$ ,  $H_2O$ , and  $CH_3OH$ . Computational studies suggest that the reorganization of  $CS_2$  upon nucleophilic attack is higher than that for  $CO_2$  and dictates the selectivity observed for frustrated Lewis pairs and could similarly apply to our system.<sup>34</sup> The electrostatic poten-

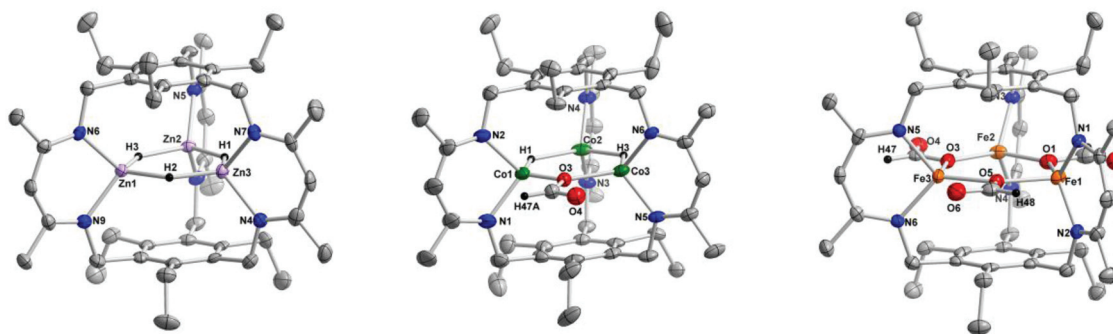


Fig. 5 Solid-State structure of  $Zn_3H_3L$  (left),  $Co_3(\mu-OCHO)(\mu-H)_2L$  (center), and  $Fe_3(\mu-OCHO)_3L$  (right) at 80%, 50%, and 80% thermal ellipsoids, respectively. Hydrogen atoms and solvent omitted for clarity (except for hydride and formate protons). C, N, Fe, Co, Zn, and O atoms depicted as gray, blue, orange, green, lavender, and red ellipsoids, and H-atoms as black spheres. Adapted from ref. 19g and i.

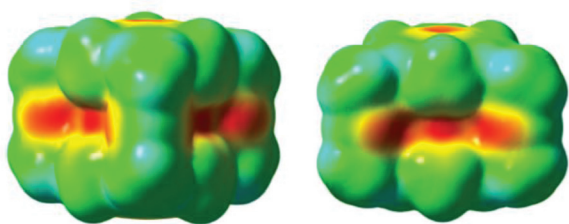


Fig. 6 Calculated electrostatic potential surface of a modified  $Zn_3H_3L$  in which ethyl groups are replaced with methyl ones. Adapted from ref. 19g.

tial surface of a modified  $Zn_3H_3L$  (*i.e.*, a methyl-for-ethyl substitution was used for computational ease) illustrates that each hydride donor is buried within a aliphatic groove (Fig. 6). The consequence of this may be that water is unreactive because approach of polar substrates to the hydride is retarded by the non-polar pocket, drawing parallels to selectivity based on substrate polarity in enzyme systems.<sup>35</sup> Previously, Holland and Schulz reported  $\beta$ -diketiminato-iron(II) and zinc(II) hydrides that crystallize as hydride-bridged dimers in the solid-state, which dissociate into the reactive monomers in solution.<sup>31,36</sup> A similar dissociative mechanism seems unlikely in our system given the structural constraints enforced by the macrobicyclic ligand. However, a fluxional bridging-to-terminal coordination mode of one or more hydrides could occur may explain the observed reactivity (*i.e.*, only one site reacts at room temperature) and slow rate of insertion into  $CO_2$  as compared to the monometallic complexes. This proposed mechanism is consistent with the difference in reactivity of  $Co_3H_3L$  and  $Fe_3H_3L$  at elevated temperatures (*viz.* the tri(formate) complex is only observed for the Fe variant). Fluxional behaviour, however, would suggest that conformations that are susceptible to reductive elimination might be accessible under the appropriate conditions. Indeed, we recently observed that  $Fe_3H_3L$  reacts with CO to eliminate  $H_2$  and generate  $[Fe(CO)]_2(FeH)L$ , which is the first isolable complex containing low-valent iron centres in this ligand.<sup>37</sup>

## Conclusions and outlook

Macrocycles have been long overlooked as potential ligands for supporting complexes for small molecule activation, with the primary role of these organic cages as selective hosts for analyte recognition. Here, we highlight the diverse reactivities and structure types of trimetallic complexes supported by one cyclophane; these compounds stabilize  $Cu(I)-N_2$  interactions at ambient temperatures and exhibit exceptional substrate specificity for hydride insertion into  $CO_2$ . As predicted, our initial studies indicate the reactivity profile of preassembled trinuclear clusters departs from that of monometallic congeners; for example,  $N_2$  cleavage upon reduction of a triiron(II) cyclophanate results in protonation of  $N_2$  derived ligands and incorporation of three N-atoms per complex. In addition, the

ability to partially metallate these ligand types hints at facile routes to probing how secondary coordination effects, and hydrogen-bonding interactions in particular, tune the reactivity of multiple metal centres; for instance, the internal cavity and hydrogen bonding partners can orient substrates in a stereospecific manner for O-atom transfer. This distinct differentiation from the monometallic and self-assembled systems bodes well for future exploration of macrobicycles with other donor arms, and opens an almost limitless landscape for potential new reactivity from the controlled design of multi-metallic compounds. In particular, the ability to readily tune the ligand sterics, such as substituting Me for Et on the benzene caps of our cyclophane, and varying the metal-metal distances, will allow us to probe the nature of selective reactivity with  $CO_2$ , the factors that influence potentially fluxional coordination of hydride donors, and the effect of metal ion type on reactivity.

## Acknowledgements

The work discussed here was supported by University of Florida, the ACS Petroleum Research Fund (ACS-PRF 52704-DNI3), and the National Science Foundation (CHE-1464876, CHE-1048604). DME was funded by the University of Florida, College of Liberal Arts and Sciences as a Graduate Research Fellowship.

## References

- 1 L. C. Seefeldt, B. M. Hoffman and D. R. Dean, *Annu. Rev. Biochem.*, 2009, **78**, 701–722.
- 2 *CRC Handbook of Chemistry and Physics*, ed. W. M. Haynes, CRC Press/Taylor and Francis, Boca Raton, FL, 2016.
- 3 H.-P. Jia and E. A. Quadrelli, *Chem. Soc. Rev.*, 2014, **43**, 547–564.
- 4 (a) J. Raymond, *Mol. Biol. Evol.*, 2003, **21**, 541–554; (b) B. M. Hoffman, D. Lukoyanov, Z.-Y. Yang, D. R. Dean and L. C. Seefeldt, *Chem. Rev.*, 2014, **114**, 4041–4062.
- 5 (a) R. Schlögl, *Angew. Chem., Int. Ed.*, 2003, **42**, 2004–2008; (b) *Catalytic Ammonia Synthesis*, ed. J. R. Jennings, Springer US, Boston, MA, 1991; (c) A. Mittasch, *Geschichte der Ammoniaksynthese*, [Weinheim (Bergstrasse)] Verlag Chemie, 1951; (d) R. Schlögl, *Ammonia Synthesis. Handbook of Heterogeneous Catalysis*, Wiley-VCH Verlag GmbH & Co. KGaA, Weinheim, Germany, 2008.
- 6 *Ullmann's Encyclopedia of Industrial Chemistry*, John Wiley & Sons, Inc., Weinheim, 7th edn, 2005.
- 7 (a) G. E. Oldroyd and R. Dixon, *Curr. Opin. Biotechnol.*, 2014, **26**, 19–24; (b) M. Han, M. Okamoto, P. H. Beatty, S. J. Rothstein and A. G. Good, *Annu. Rev. Genet.*, 2015, **49**, 269–289; (c) B. A. Geddes, M.-H. Ryu, F. Mus, A. Garcia Costas, J. W. Peters, C. A. Voigt and P. Poole, *Curr. Opin. Biotechnol.*, 2015, **32**, 216–222.

- 8 (a) S. Ramaswamy, *Science*, 2011, **334**, 914–915; (b) T. Spatzal, M. Aksoyoglu, L. Zhang, S. L. A. Andrade, E. Schleicher, S. Weber, D. C. Rees and O. Einsle, *Science*, 2011, **334**, 940–940; (c) K. M. Lancaster, M. Roemelt, P. Ettenhuber, Y. Hu, M. W. Ribbe, F. Neese, U. Bergmann and S. DeBeer, *Science*, 2011, **334**, 974–977.
- 9 (a) T. I. Doukov, *Science*, 2002, **298**, 567–572; (b) J.-H. Jeoung and H. Dobbek, *Science*, 2007, **318**, 1461–1464; (c) T. Haltia, K. Brown, M. Tegoni, C. Cambillau, M. Saraste, K. Mattila and K. Djinovic-Carugo, *Biochem. J.*, 2003, **369**, 77–88; (d) E. M. Johnston, S. Dell'Acqua, S. Ramos, S. R. Pauleta, I. Moura and E. I. Solomon, *J. Am. Chem. Soc.*, 2014, **136**, 614–617; (e) K. Paraskevopoulos, S. V. Antonyuk, R. G. Sawers, R. R. Eady and S. S. Hasnain, *J. Mol. Biol.*, 2006, **362**, 55–65; (f) C. L. Drennan, J. Heo, M. D. Sintchak, E. Schreiter and P. W. Ludden, *Proc. Natl. Acad. Sci. U. S. A.*, 2001, **98**, 11973–11978; (g) A. Pomowski, W. G. Zumft, P. M. H. Kroneck and O. Einsle, *Nature*, 2011, **477**, 234–237; (h) T. Rasmussen, B. C. Berks, J. Sanders-Loehr, D. M. Dooley, W. G. Zumft and A. J. Thomson, *Biochemistry*, 2000, **39**, 12753–12756.
- 10 (a) L. J. Clouston, V. Bernales, R. K. Carlson, L. Gagliardi and C. C. Lu, *Inorg. Chem.*, 2015, **54**, 9263–9270; (b) P. A. Rudd, N. Planas, E. Bill, L. Gagliardi and C. C. Lu, *Eur. J. Inorg. Chem.*, 2013, **2013**, 3898–3906; (c) R. B. Siedschlag, V. Bernales, K. D. Vogiatzis, N. Planas, L. J. Clouston, E. Bill, L. Gagliardi and C. C. Lu, *J. Am. Chem. Soc.*, 2015, **137**, 4638–4641; (d) B. P. Greenwood, G. T. Rowe, C.-H. Chen, B. M. Foxman and C. M. Thomas, *J. Am. Chem. Soc.*, 2010, **132**, 44–45; (e) B. Wu, K. M. Gramigna, M. W. Bezpalko, B. M. Foxman and C. M. Thomas, *Inorg. Chem.*, 2015, **54**, 10909–10917; (f) T. M. Powers, A. R. Fout, S.-L. Zheng and T. A. Betley, *J. Am. Chem. Soc.*, 2011, **133**, 3336–3338; (g) T. M. Powers and T. A. Betley, *J. Am. Chem. Soc.*, 2013, **135**, 12289–12296; (h) T. D. Harris and T. A. Betley, *J. Am. Chem. Soc.*, 2011, **133**, 13852–13855; (i) S. E. Creutz and J. C. Peters, *J. Am. Chem. Soc.*, 2015, **137**, 7310–7313; (j) M. Nippe, S. M. Goodman, C. G. Fry and J. F. Berry, *J. Am. Chem. Soc.*, 2011, **133**, 2856–2859; (k) D. W. Brogden, Y. Turov, M. Nippe, G. L. Manni, E. A. Hillard, R. Clérac, L. Gagliardi and J. F. Berry, *Inorg. Chem.*, 2014, **53**, 4777–4790.
- 11 A. D. Allen and C. V. Senoff, *Chem. Commun.*, 1965, 621–622.
- 12 C. E. Laplaza and C. C. Cummins, *Science*, 1995, **268**, 861–863.
- 13 M. D. Fryzuk, *Science*, 1997, **275**, 1445–1447.
- 14 D. V. Yandulov, *Science*, 2003, **301**, 76–78.
- 15 K. Arashiba, Y. Miyake and Y. Nishibayashi, *Nat. Chem.*, 2011, **3**, 120–125.
- 16 J. D. Gilbertson, N. K. Szymczak and D. R. Tyler, *J. Am. Chem. Soc.*, 2005, **127**, 10184–10185.
- 17 M. M. Rodriguez, E. Bill, W. W. Brennessel and P. L. Holland, *Science*, 2011, **334**, 780–783.
- 18 (a) T. A. Betley and J. C. Peters, *J. Am. Chem. Soc.*, 2004, **126**, 6252–6254; (b) A. Takaoka, N. P. Mankad and J. C. Peters, *J. Am. Chem. Soc.*, 2011, **133**, 8440–8443; (c) J. S. Anderson, J. Rittle and J. C. Peters, *Nature*, 2013, **501**, 84–87; (d) S. E. Creutz and J. C. Peters, *J. Am. Chem. Soc.*, 2014, **136**, 1105–1115; (e) J. S. Anderson, G. E. Cutsail III, J. Rittle, B. A. Connor, W. A. Gunderson, L. Zhang, B. M. Hoffman and J. C. Peters, *J. Am. Chem. Soc.*, 2015, **137**, 7803–7809; (f) J. Rittle and J. C. Peters, *J. Am. Chem. Soc.*, 2016, **138**, 4243–4248.
- 19 (a) G. L. Guillet, F. T. Sloane, M. F. Dumont, K. A. Abboud and L. J. Murray, *Dalton Trans.*, 2012, **41**, 7866; (b) G. L. Guillet, J. B. Gordon, G. N. Di Francesco, M. W. Calkins, E. Čižmár, K. A. Abboud, M. W. Meisel, R. García-Serres and L. J. Murray, *Inorg. Chem.*, 2015, **54**, 2691–2704; (c) G. L. Guillet, F. T. Sloane, D. M. Ermert, M. W. Calkins, M. K. Peprah, E. S. Knowles, E. Čižmár, K. A. Abboud, M. W. Meisel and L. J. Murray, *Chem. Commun.*, 2013, **49**, 6635; (d) G. N. Di Francesco, A. Gaillard, I. Ghiviriga, K. A. Abboud and L. J. Murray, *Inorg. Chem.*, 2014, **53**, 4647–4654; (e) L. J. Murray, W. W. Weare, J. Shearer, A. D. Mitchell and K. A. Abboud, *J. Am. Chem. Soc.*, 2014, **136**, 13502–13505; (f) Y. Lee, F. T. Sloane, G. Blondin, K. A. Abboud, R. García-Serres and L. J. Murray, *Angew. Chem., Int. Ed.*, 2015, **54**, 1499–1503; (g) D. M. Ermert, I. Ghiviriga, V. J. Catalano, J. Shearer and L. J. Murray, *Angew. Chem., Int. Ed.*, 2015, **54**, 7047–7050; (h) D. M. Ermert, J. B. Gordon, K. A. Abboud and L. J. Murray, *Inorg. Chem.*, 2015, **54**, 9282–9289; (i) Y. Lee, K. J. Anderton, F. T. Sloane, D. M. Ermert, K. A. Abboud, R. García-Serres and L. J. Murray, *J. Am. Chem. Soc.*, 2015, **137**, 10610–10617; (j) Y. Lee, I.-R. Jeon, K. A. Abboud, R. García-Serres, J. Shearer and L. J. Murray, *Chem. Commun.*, 2016, **52**, 1174–1177; (k) D. M. Ermert, J. B. Gordon, K. A. Abboud and L. J. Murray, Submitted.
- 20 (a) P. Mateus, R. Delgado, F. Lloret, J. Cano, P. Brandão and V. Félix, *Chem. – Eur. J.*, 2011, **17**, 11193–11203; (b) E. Zysman-Colman and C. Denis, *Coord. Chem. Rev.*, 2012, **256**, 1742–1761.
- 21 G. Hennrich and E. V. Anslyn, *Chem. – Eur. J.*, 2002, **8**, 2218–2224.
- 22 M. Hashizume, S. Tobey, V. M. Lynch and E. V. Anslyn, *Supramol. Chem.*, 2002, **14**, 511–517.
- 23 (a) Y.-C. Tsai, *Coord. Chem. Rev.*, 2012, **256**, 722–758; (b) V. T. Annibale and D. Song, *RSC Adv.*, 2013, **3**, 11432–11449; (c) C. Chen, S. M. Bellows and P. L. Holland, *Dalton Trans.*, 2015, **44**, 16654–16670.
- 24 (a) D. E. Heppner, C. H. Kjaergaard and E. I. Solomon, *J. Am. Chem. Soc.*, 2013, **135**, 12212–12215; (b) E. I. Solomon, U. M. Sundaram and T. E. Machonkin, *Chem. Rev.*, 1996, **96**, 2563–2606; (c) E. I. Solomon, A. J. Augustine and J. Yoon, *Dalton Trans.*, 2008, **30**, 3921–3932; (d) A. B. Taylor, C. S. Stoj, L. Ziegler, D. J. Kosman and P. J. Hart, *Proc. Natl. Acad. Sci. U. S. A.*, 2005, **102**, 15459–15464.
- 25 (a) J. T. York, I. Bar-Nahum and W. B. Tolman, *Inorg. Chem.*, 2007, **46**, 8105–8107; (b) E. C. Brown, I. Bar-Nahum, J. T. York, N. W. Aboeella and W. B. Tolman, *Inorg. Chem.*, 2007, **46**, 486–496.

- 26 (a) Y. Kuroda, Y. Yoshikawa, S. Emura, R. Kumashiro and M. Nagao, *J. Phys. Chem. B*, 1999, **103**, 2155–2164; (b) C. L. Gatlin, F. Tureček and T. Vaisar, *J. Mass Spectrom.*, 1995, **30**, 775–777; (c) G. Spoto, S. Bordiga, G. Ricchiardi, D. Scarano, A. Zecchina and F. Geobaldo, *J. Chem. Soc., Faraday Trans.*, 1995, **91**, 3285–3290; (d) H. S. Plitt, H. Schnöckel, M. Bär and R. Ahlrichs, *Z. Anorg. Allg. Chem.*, 1992, **607**, 45–51; (e) S. G. Francis, S. L. Matthews, O. K. Poleshchuk, N. R. Walker and A. C. Legon, *Angew. Chem., Int. Ed.*, 2006, **45**, 6341–6343; (f) Y. Kuroda, Y. Yoshikawa, S. Konno, H. Hamano, H. Maeda, R. Kumashiro and M. Nagao, *J. Phys. Chem.*, 1995, **99**, 10621–10628; (g) Y. Kuroda, S.-I. Konno, K. Morimoto and Y. Yoshikawa, *J. Chem. Soc., Chem. Commun.*, 1993, **1**, 18–20.
- 27 T. M. Figg, P. L. Holland and T. R. Cundari, *Inorg. Chem.*, 2012, **51**, 7546–7550.
- 28 (a) J. M. Smith, R. J. Lachicotte, K. A. Pittard, T. R. Cundari, G. Lukat-Rodgers, K. R. Rodgers and P. L. Holland, *J. Am. Chem. Soc.*, 2001, **123**, 9222–9223; (b) J. M. Smith, A. R. Sadique, T. R. Cundari, K. R. Rodgers, G. Lukat-Rodgers, R. J. Lachicotte, C. J. Flaschenriem, J. Vela and P. L. Holland, *J. Am. Chem. Soc.*, 2006, **128**, 756–769.
- 29 D. Lukoyanov, N. Khadka, Z.-Y. Yang, D. R. Dean, L. C. Seefeldt and B. M. Hoffman, *J. Am. Chem. Soc.*, 2016, **138**, 1320–1327.
- 30 (a) T. Shima, S. Hu, G. Luo, X. Kang, Y. Luo and Z. Hou, *Science*, 2013, **340**, 1549–1552; (b) J. Ballmann, R. F. Munhá and M. D. Fryzuk, *Chem. Commun.*, 2010, **46**, 1013.
- 31 Y. Yu, A. R. Sadique, J. M. Smith, T. R. Dugan, R. E. Cowley, W. W. Brennessel, C. J. Flaschenriem, E. Bill, T. R. Cundari and P. L. Holland, *J. Am. Chem. Soc.*, 2008, **130**, 6624–6638.
- 32 B. M. Hoffman, D. Lukoyanov, D. R. Dean and L. C. Seefeldt, *Acc. Chem. Res.*, 2013, **46**, 587–595.
- 33 (a) S. Enthaler, *ACS Catal.*, 2013, **3**, 150–158; (b) H. C. Brown and P. V. Ramachandran, in *Reductions in Organic Synthesis*, ed. A. F. Abdel-Magid, American Chemical Society, Washington, DC, 1996, ch. 1, pp. 1–30; (c) X.-F. Wu, *Chem. – Asian J.*, 2012, **7**, 2502–2509; (d) C. Boone, I. Korobkov and G. I. Nikonov, *ACS Catal.*, 2013, **3**, 2336–2340; (e) G. Bendt, S. Schulz, J. Spielmann, S. Schmidt, D. Bläser and C. Wölper, *Eur. J. Inorg. Chem.*, 2012, 3725–3731.
- 34 K. An and J. Zhu, *Organometallics*, 2014, **33**, 7141–7146.
- 35 A. Warshel, P. K. Sharma, M. Kato, Y. Xiang, H. Liu and M. H. M. Olsson, *Chem. Rev.*, 2006, **106**, 3210–3235.
- 36 (a) S. Schulz, T. Eisenmann, S. Schmidt, D. Bläser, U. Westphal and R. Boese, *Chem. Commun.*, 2010, **46**, 7226; (b) J. M. Smith, R. J. Lachicotte and P. L. Holland, *J. Am. Chem. Soc.*, 2003, **125**, 15752–15753.
- 37 K. J. Anderton, K. A. Abboud, R. García-Serres and L. J. Murray, submitted.
- 38 K. C. MacLeod, S. F. McWilliams, B. Q. Mercado and P. L. Holland, *Chem. Sci.*, 2016, DOI: 10.1039/c6sc00423g.